

# Tkachenko Modes of Vortex Lattices in Rapidly Rotating Bose-Einstein Condensates

Gordon Baym

*Department of Physics, University of Illinois at Urbana-Champaign, 1110 West Green Street, Urbana, Illinois 61801, USA*  
(Received 13 May 2003; published 9 September 2003)

We calculate the in-plane modes of the vortex lattice in a rotating Bose condensate, from the slowly rotating to mean-field quantum Hall limits. The Tkachenko mode frequency, linear in wave vector  $k$  for lattice rotational velocities  $\Omega$  much smaller than the lowest sound wave frequency in a finite system, becomes quadratic in  $k$  in the opposite limit. The system also supports an inertial mode of frequency  $\geq 2\Omega$ . The calculated frequencies are in excellent agreement with recent observations of Tkachenko modes by I. Coddington, P. Engels, V. Schweikhard, and E. A. Cornell, *Phys. Rev. Lett.* **91**, 100402 (2003).

DOI: 10.1103/PhysRevLett.91.110402

PACS numbers: 03.75.Hh, 05.30.Jp, 67.40.Db, 67.40.Vs

The collective modes of the vortex lattice in a rotating superfluid have been of considerable interest since the 1960s. In a classic series of papers Tkachenko [1] showed that the lattice supports an elliptically polarized oscillatory mode, a mode observed in superfluid helium in 1982 [2]. Reference [3] reformulated the hydrodynamics of rotating superfluids to take into account the elasticity of the vortex lattice (including normal fluid, dissipation, and line bending—Kelvin—oscillations of the vortex lines in three dimensions) and thus describe the Tkachenko modes; effects of the oscillations of the vortex lines at finite temperature on the long range phase correlations of the superfluid were discussed in [4]. The focus of these papers was on superfluid helium, where rotational speeds are always much smaller than characteristic phonon frequencies ( $\geq$  MHz).

Atomic Bose condensates, on the other hand, allow one to study superfluids over a large range of rotational frequencies,  $\Omega$  [5–9]. We identify four distinct physical regimes in a trapped condensate as  $\Omega$  increases: (i) The “stiff” Thomas-Fermi regime, where  $\Omega$  is small compared with the lowest compressional frequencies,  $sk_0$ , where  $s$  is the sound velocity,  $k_0 \sim 1/R$  is the lowest wave number in the finite geometry, and  $R$  is the size of the system transverse to the rotation axis. In this regime the system responds to rotation effectively as an incompressible fluid. (ii) At larger  $\Omega$ ,  $\gg sk_0$ —but  $\ll ms^2$  ( $m$  is the atomic mass), or equivalently, vortex core size still small compared with the intervortex spacing—the system is in the “soft” Thomas-Fermi regime, where compression of the superfluid becomes important in the response of the lattice. Such effects, taken into account here for the first time, are primarily responsible for bringing theory into agreement with experiment. (iii) When  $\Omega \gg ms^2$ , a condensate in a harmonic trap flattens to a very weakly interacting effectively two-dimensional system, and rotational speeds can well exceed phonon frequencies. The system enters the “mean field” quantum Hall regime, in which the condensation is only in lowest Landau orbits [10]. Here corrections to the elastic

shear modulus of the vortex lattice are important. (iv) Eventually the vortex lattice melts [11,12], and the system enters a strongly correlated regime [14–16].

Tkachenko modes in Bose-condensed  $^{87}\text{Rb}$  were recently observed by Coddington *et al.* [17] at rotation speeds up to 0.975 of the transverse trapping frequency,  $\omega_\rho$ ; in this regime,  $\Omega$  increases past  $sk_0$ , and although not yet in the quantum Hall regime, the experiments show effects of very rapid rotation on the mode frequencies. The modes in rotating atomic condensates have also been the subject of several theoretical investigations. Reference [17] determined the Tkachenko modes at slow rotation in trapping geometry, but not including effects of compressibility significantly overestimated the mode frequencies in the soft regime [17]. The fundamental modes in trapping geometry in the absence of the elastic energy of the lattice were determined in [18]. Studies in the quantum Hall regime are given in [12, 19–21]. In this Letter we derive the modes of the vortex lattice in a Bose condensate at general  $\Omega/\omega_\rho < 1$ . The present analysis is restricted to long wavelength linearized motion in two dimensions transverse to the rotation axis, at zero temperature [23]. We work only to needed leading orders in  $k$ . The starting point is the conservation laws and superfluid acceleration equation governing the system, including the full elasticity of the lattice. We generally assume a gas of bosons with a short range repulsive interaction,  $U(r) = g\delta^3(r)$ , where  $g = 4\pi a_s/m$ ,  $a_s$  is the  $s$ -wave scattering length, and  $\hbar = 1$ .

The angular momentum of the superfluid is carried in vortices, which form a triangular lattice rotating as a solid body at angular velocity  $\Omega$ . We work in the frame corotating with the vortex lattice, and denote the deviations of the vortices from their home positions by the continuum displacement field,  $\epsilon(r, t)$ . In linear order, the long wavelength superfluid velocity,  $v(r, t)$ , can be written, following [4], in terms of  $\epsilon(r, t)$ , and the phase  $\Phi(r, t)$  of the order parameter, as

$$v + 2\Omega \times \epsilon = \nabla\Phi/m. \quad (1)$$

This equation follows from the fact that its curl,

$$\nabla \times \mathbf{v} = -2\Omega \nabla \cdot \boldsymbol{\epsilon}, \quad (2)$$

is the conservation law relating the change in vorticity to a compression of the vortex lattice, while its longitudinal part is trivially the gradient of a scalar [24]. Equation (2) constrains the number of degrees of freedom in two dimensions from five ( $n, \mathbf{v}, \boldsymbol{\epsilon}$ ) to four. The time derivative of Eq. (1) is the superfluid acceleration equation,

$$m \left( \frac{\partial \mathbf{v}}{\partial t} + 2\Omega \times \dot{\boldsymbol{\epsilon}} \right) = -\nabla(\mu - V_{\text{eff}}), \quad (3)$$

where for a harmonic confining trap in two dimensions,

$$V_{\text{eff}} = \frac{m}{2} \left( \omega_\rho^2 - \Omega^2 \right) r^2; \quad (4)$$

$\mu$  is the chemical potential, related in the rotating frame to the phase by  $\mu(r, t) - V_{\text{eff}} = -(1/m)\partial\Phi(r, t)/\partial t$ .

The local elastic energy density of a triangular lattice in two dimensions has the form [3]

$$\mathcal{E}(r) = 2C_1(\nabla \cdot \boldsymbol{\epsilon})^2 + C_2 \left[ \left( \frac{\partial \epsilon_x}{\partial x} - \frac{\partial \epsilon_y}{\partial y} \right)^2 + \left( \frac{\partial \epsilon_x}{\partial y} + \frac{\partial \epsilon_y}{\partial x} \right)^2 \right], \quad (5)$$

where  $C_1$  is the compressional modulus and  $C_2$  is the shear modulus of the vortex lattice. In an incompressible fluid,  $C_2 = \Omega n/8 = -C_1$  [1,3]. The shear modulus increases with increasing  $\Omega$ , eventually reaching, in the mean-field quantum Hall limit [12,22],  $C_2 \simeq (81/80\pi^4)ms^2n$ . The falloff for small  $\Omega/ms^2$  has the form

$$C_2 \simeq \frac{\Omega n}{8} \left( 1 - \gamma \frac{\Omega}{ms^2} + \dots \right); \quad (6)$$

a first estimate [22] is  $\gamma \sim 4$ .

The dynamics is specified by the superfluid acceleration equation (3); the continuity equation,

$$\frac{\partial n(r, t)}{\partial t} + \nabla \cdot \mathbf{j}(r, t) = 0, \quad (7)$$

where  $n$  is the (smoothed) density, and  $\mathbf{j} = n\mathbf{v}$  is the particle current; and conservation of momentum,

$$D(k, \omega) \equiv \omega^4 - \omega^2 \left[ 4\Omega^2 + \left( s^2 + \frac{4}{nm}(C_1 + C_2) \right) k^2 \right] + \frac{2s^2C_2}{nm} k^4 = (\omega^2 - \omega_I^2)(\omega^2 - \omega_T^2) = 0. \quad (14)$$

For  $2s^2C_2k^4/nm \ll \{4\Omega^2 + [s^2 + 4(C_1 + C_2)/nm]k^2\}^2$ , as is generally the case, the mode frequencies are given by

$$\omega_I^2 = 4\Omega^2 + \left( s^2 + \frac{4}{nm}(C_1 + C_2) \right) k^2 \quad (15)$$

and

$$\omega_T^2 = \frac{2C_2}{nm} \frac{s^2k^4}{\{4\Omega^2 + [s^2 + 4(C_1 + C_2)/nm]k^2\}}. \quad (16)$$

$$m \left( \frac{\partial \mathbf{j}}{\partial t} + 2\Omega \times \mathbf{j} \right) + \nabla P + n \nabla V_{\text{eff}} = -\boldsymbol{\sigma}, \quad (8)$$

where  $P$  is the pressure. At zero temperature and long wavelengths,  $\nabla P = n \nabla \mu = ms^2 \nabla n$ , where  $s$  is the sound velocity [25]; in equilibrium,  $\nabla P + n \nabla V_{\text{eff}} = 0$ . The elastic stress,  $\boldsymbol{\sigma}$ , is given in terms of the total elastic energy,  $E_{\text{el}} = \int d^2r \mathcal{E}(r)$ , by

$$\boldsymbol{\sigma}(r, t) = \frac{\delta E_{\text{el}}}{\delta \boldsymbol{\epsilon}} = -4C_1 \nabla(\nabla \cdot \boldsymbol{\epsilon}) - 2C_2 \nabla^2 \boldsymbol{\epsilon}. \quad (9)$$

Equations (8) and (3), with  $\nabla P = n \nabla \mu$ , imply  $2\Omega \times (\dot{\boldsymbol{\epsilon}} - \mathbf{v}) = \boldsymbol{\sigma}/mn$ . The curl of this equation becomes

$$\nabla \cdot (\dot{\boldsymbol{\epsilon}} - \mathbf{v}) = \frac{\nabla \times \boldsymbol{\sigma}}{2\Omega nm} = \frac{C_2}{\Omega nm} \nabla^2 (\nabla \times \boldsymbol{\epsilon}), \quad (10)$$

while its divergence, together with (2), yields

$$\nabla \times \dot{\boldsymbol{\epsilon}} + 2\Omega \nabla \cdot \boldsymbol{\epsilon} = -\frac{\nabla \cdot \boldsymbol{\sigma}}{2\Omega nm} = \frac{C_2 + 2C_1}{\Omega nm} \nabla^2 (\nabla \cdot \boldsymbol{\epsilon}). \quad (11)$$

The structure of the modes follows directly from the linearized set of equations, (2), (10), and (11), and the divergence of (3). The density oscillations are governed by

$$\left( -\frac{\partial^2}{\partial t^2} + s^2 \nabla^2 \right) n = 2n\Omega \nabla \times \dot{\boldsymbol{\epsilon}}. \quad (12)$$

Using Eq. (10) to eliminate  $\nabla \times \boldsymbol{\epsilon}$ , and dropping the higher order term  $\sim \nabla^4$ , we find

$$\left( -\frac{\partial^2}{\partial t^2} + \frac{2C_2}{mn} \nabla^2 \right) \nabla \cdot \boldsymbol{\epsilon} = \frac{1}{n} \frac{\partial^2}{\partial t^2} n. \quad (13)$$

In the absence of coupling of density oscillations to compressions of the vortex lattice, Eq. (12) is simply that of long wavelength phonons in the condensate [27], while Eq. (13) describes Tkachenko modes of the vortex lattice [1,3,4] of wave vector  $k$  and frequency  $\omega_T = (2C_2/mn)^{1/2}k$ .

The coupled Eqs. (12) and (13) yield the full spectrum of long wavelength modes. The frequencies, for given  $k$ , are solutions of the secular equation

The first mode is the standard inertial mode of a rotating fluid; for  $\Omega \ll s^2k^2$  it is a sound wave, while for  $\Omega \gg s^2k^2$  the mode frequencies begin essentially at  $2\Omega$ . The second mode is the elliptically polarized Tkachenko mode observed in [16]. See Fig. 1. As Eq. (11) implies, the longitudinally polarized component is  $\pi/2$  out of phase with the transversely polarized component, of order  $\omega_T/2\Omega$  smaller for the Tkachenko mode and of similar

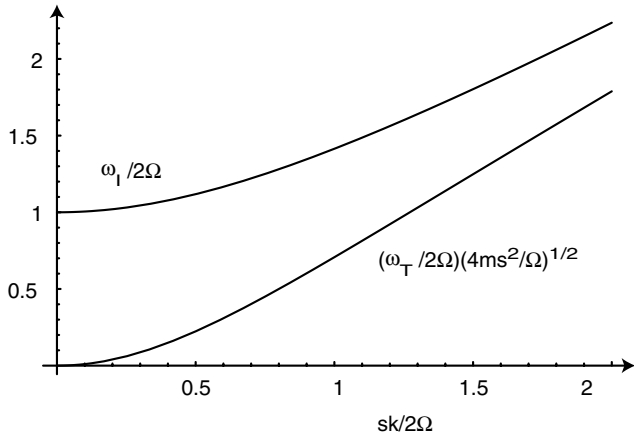


FIG. 1. Inertial and Tkachenko mode frequencies vs wave vector, in units of  $2\Omega/s$ . The inertial mode frequency (upper curve) is in units of  $2\Omega$ , while the Tkachenko frequency (lower curve) is in units of  $(\Omega^3/ms^2)^{1/2}$ . The frequencies shown are for  $\Omega \ll ms^2$ ; in the quantum Hall regime, the Tkachenko modes are softer by a factor  $(9/\pi^2)(ms^2/10\Omega)^{1/2}$ .

size for the inertial mode [28]. The forms of the mode frequencies do not depend on the system being weakly interacting. In the stiff limit, the Tkachenko frequency,  $\omega_T = (\Omega/4m)^{1/2}k$ , is linear in  $k$ . By contrast, in the soft limit, the mode frequency  $\omega_T$  is quadratic in  $k$  at long wavelengths,

$$\omega_T = \left(\frac{C_2}{2nm}\right)^{1/2} \frac{sk^2}{\Omega}; \quad (17)$$

in the quantum Hall limit,  $\omega_T \simeq (9/4\pi^2\sqrt{10}) \times (s^2k^2/\Omega)$  [12].

The softness of the Tkachenko modes in the rapidly rotating regime leads to infrared singular behavior in the vortex transverse displacement-displacement correlations at finite temperature, and in the order parameter phase correlations even at zero temperature [12,13]. In a finite system the single particle density matrix,  $\langle\psi(r)\psi^\dagger(r')\rangle$ , falls algebraically as  $|\vec{r} - \vec{r}'|^{-\eta}$ , where  $\eta \simeq (ms^2n/8C_2)^{1/2}N_v/N$ ,  $N_v$  is the total number of vortices present, and  $N$  is the total particle number [13]. Dephasing of the condensate becomes significant only as  $N_v \rightarrow N$ , and not necessarily before the vortex lattice melts.

To compare Eq. (16) with the experiment of Ref. [16], we extract the effective value of  $k$  in the lowest Tkachenko mode from the numerical result of Ref. [17] for the fundamental frequency:  $\omega_T \simeq 1.43a\Omega/R = 2.72(\Omega/m)^{1/2}/R$ , where  $a = (2\pi)^{1/2}/3^{1/4}(m\Omega)^{1/2}$  is the lattice constant, and  $R$  the transverse Thomas-Fermi radius. Comparison with the slow rotation Tkachenko frequency,  $(\Omega/4m)^{1/2}k$ , implies an effective wave vector of the lowest mode,  $k_0 = \alpha/R$ , where  $\alpha \simeq 5.45$ . Tacitly assuming the mode function of [17], we use this value of  $k$  in the following. Corrections at high  $\Omega$  to the mode function remain to be determined. The transverse

Thomas-Fermi radius of a rotating condensate is given by [25]  $R^2 = d^2\tau(1-x)^{-3/5}$ , where  $x = \Omega^2/\omega_\rho^2$ ,  $d = 1/(m\omega_\rho)^{1/2}$  is the transverse oscillator length,  $\tau = [(15Nb a_s/d)(\omega_z/\omega_\rho)]^{2/5}$ , and  $\omega_z$  is the axial trapping frequency. The sound velocity in the center of the trap is  $ms(0)^2 = gbn(0) = (\omega_\rho/2)\tau(1-x)^{2/5}$ , so that

$$\frac{\Omega}{ms(0)^2} = \frac{2}{\tau} \frac{x^{1/2}}{(1-x)^{2/5}}. \quad (18)$$

Also,  $[\Omega/s(0)k_0]^2 = 2x/(1-x)\alpha^2$ ; in the present experiments,  $\Omega/s(0)k_0$  reaches  $\sim 1.15$ . Ignoring  $b \simeq 1$  here [25], as well as the small  $C_1 + C_2$  term in (16), we have

$$\omega_T^2 = \omega_\rho^2 \left(\frac{C_2}{\Omega n/8}\right) \frac{\alpha^2}{4\tau} \frac{x^{1/2}(1-x)^{8/5}}{1-x\{1 - (8/\alpha^2)[s(0)^2/\bar{s}^2]\}}, \quad (19)$$

where  $\bar{s}^2$  is the sound velocity squared appropriately averaged over the mode function. In the mean-field quantum Hall regime,  $\omega_T/\omega_\rho \sim (1-x)$ .

The inset of Fig. 2 shows the Tkachenko mode frequencies as a function of  $\Omega/\omega_\rho$ , illustrating the initial square root rise and the eventual falloff for  $\Omega \lesssim \omega_\rho$ . The curves are evaluated for the parameters of Ref. [16],  $(\omega_\rho, \omega_z) = 2\pi(8.3, 5.2)$  Hz, at the representative condensate number,  $N = 2.5 \times 10^6$ . Figure 2 proper shows these curves in the region measured in [16]. The upper curve is calculated from Eq. (19) with  $\bar{s}^2 = s(0)^2$ . The experiments of [16] (triangles) are at  $N \sim (0.7-3) \times 10^6$ . According to (19), the frequencies scale as  $N^{-1/5}$ ; thus to facilitate comparison with theory, shown for  $N = 2.5 \times 10^6$ , we have scaled the individual data points down by a factor  $(N/2.5 \times 10^6)^{1/5}$ , equivalent to scaling the theory up by

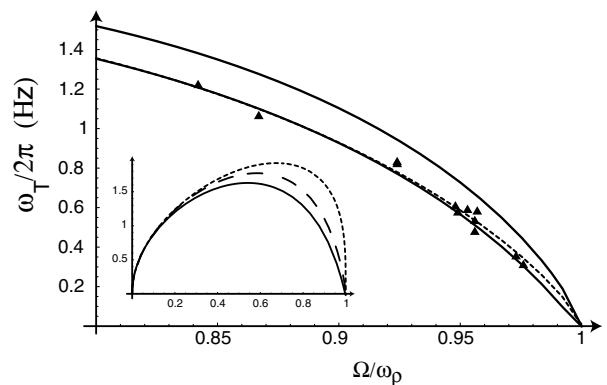


FIG. 2. Frequency of the lowest Tkachenko mode. The upper curve is evaluated at constant shear modulus,  $C_2$ , and the central sound velocity. The lower solid curve includes a decreasing  $C_2$ , Eq. (6) with  $\gamma = 4$ ; in the dashed curve  $\bar{s}^2/s(0)^2 = 4/7$  with  $\gamma = 0$ . Note that the solid curve falls below the dashed curve at high  $\Omega$ . The data (triangles) from Ref. [16] are multiplied by a factor  $(N/2.5 \times 10^6)^{-1/5}$  to compare with theory, calculated for  $N = 2.5 \times 10^6$ . The inset shows  $\omega_T$  over the entire range of  $\Omega$ ; the upper (short dashed) curve is the mode frequency to lowest order in the wave vector [18]; the lower curves include the full  $k$  dependence at constant  $C_2$ , and  $\bar{s}^2/s(0)^2 = 1$  (dashed curve) and  $4/7$  (solid curve).

the same factor. For  $\Omega \gtrsim sk_0$ , inclusion of the effects of compressibility brings the theory much closer to experiment. Two further effects enter into producing final agreement with the data. The first is to replace the central sound velocity by the lower  $\bar{s}^2$ . A simple approximation [29] is to use the density weighted average  $\bar{s}^2 = \int n(r) s(r)^2 / \int n(r) = (4/7)s(0)^2$  for a Thomas-Fermi structure. The second effect is the softening of  $C_2$  at higher rotation. The theory with  $\bar{s}^2/s(0)^2 = 4/7$  and no softening (dashed lower curve) or with  $\bar{s}^2/s(0)^2 = 1$  and softening given by  $\gamma = 4$  (solid lower curve) yield predictions indistinguishable for present rotations, and in excellent agreement with the data. However, as Fig. 2 shows, the drop of  $C_2/\Omega$  with increasing  $\Omega$  produces a noticeable decrease in  $\omega_T$  for  $\Omega$  within a few percent of  $\omega_\rho$ ; clear evidence for the falloff of  $C_2/\Omega$  emerges from yet higher frequency data [29].

I am grateful to Eric Cornell, Ian Coddington, Peter Engels, and Volker Schweikhard for helpful discussions and for giving me permission to include the JILA data here. I also thank Sandro Stringari, Marco Cozzini, and Drew Gifford for useful conversations. This work was supported in part by NSF Grant No. PHY00-98353.

- 
- [1] V.K. Tkachenko, Zh. Eksp. Teor. Fiz. **49**, 1875 (1965) [Sov. Phys. JETP **22**, 1282 (1966)]; Zh. Eksp. Teor. Fiz. **50**, 1573 (1966) [Sov. Phys. JETP **23**, 1049 (1966)]; Zh. Eksp. Teor. Fiz. **56**, 1763 (1969) [Sov. Phys. JETP **29**, 245 (1969)].
- [2] C. D. Andereck and W. I. Glaberson, J. Low Temp. Phys. **48**, 257 (1982).
- [3] G. Baym and E. Chandler, J. Low Temp. Phys. **50**, 57 (1983); **62**, 119 (1986).
- [4] G. Baym, Phys. Rev. B **51**, 11 697 (1995).
- [5] M. R. Matthews, B. P. Anderson, P. C. Haljan, D. S. Hall, C. E. Wieman, and E. A. Cornell, Phys. Rev. Lett. **83**, 2498 (1999).
- [6] K. W. Madison, F. Chevy, W. Wohlleben, and J. Dalibard, Phys. Rev. Lett. **84**, 806 (2000); F. Chevy, K. W. Madison, and J. Dalibard, Phys. Rev. Lett. **85**, 2223 (2000); K. W. Madison, F. Chevy, V. Bretin, and J. Dalibard, Phys. Rev. Lett. **86**, 4443 (2001); V. Bretin, S. Stock, Y. Seurin, and J. Dalibard, cond-mat/0307464.
- [7] J. R. Abo-Shaeer, C. Raman, J. M. Vogels, and W. Ketterle, Science **292**, 476 (2001).
- [8] P. C. Haljan, I. Coddington, P. Engels, and E. A. Cornell, Phys. Rev. Lett. **87**, 210403 (2001); P. Engels, I. Coddington, P. C. Haljan, and E. A. Cornell, Phys. Rev. Lett. **89**, 100403 (2002).
- [9] A. E. Leanhardt, A. Görlitz, A. P. Chikkatur, D. Kielpinski, Y. Shin, D. E. Pritchard, and W. Ketterle, Phys. Rev. Lett. **89**, 190403 (2002).
- [10] T.-L. Ho, Phys. Rev. Lett. **87**, 060403 (2001).
- [11] A. Rozhkov and D. Stroud, Phys. Rev. B **54**, R12 697 (1996).
- [12] J. Sinova, C. B. Hanna, and A. H. MacDonald, Phys. Rev. Lett. **89**, 030403 (2002).
- [13] G. Baym, cond-mat/0308342.
- [14] N. K. Wilkin, J. M. F. Gunn, and R. A. Smith, Phys. Rev. Lett. **80**, 2265 (1998); N. K. Wilkin and J. M. F. Gunn, Phys. Rev. Lett. **84**, 6 (2000); N. R. Cooper, N. K. Wilkin, and J. M. F. Gunn, Phys. Rev. Lett. **87**, 120405 (2001).
- [15] S. Viefers, T. H. Hansson, and S. M. Reimann, Phys. Rev. A **62**, 053604 (2000).
- [16] N. Regnault and Th. Jolicoeur, cond-mat/0212477.
- [17] I. Coddington, P. Engels, V. Schweikhard, and E. A. Cornell, Phys. Rev. Lett. **91**, 100402 (2003).
- [18] J. R. Anglin and M. Crescimanno, cond-mat/0210063.
- [19] M. Cozzini and S. Stringari, Phys. Rev. A **67**, 041602 (2003).
- [20] M. Cozzini, L. Pitaevskii, and S. Stringari (to be published).
- [21] M. A. Cazalilla, cond-mat/0207715.
- [22] G. Baym (to be published).
- [23] At finite  $T$ , the normal fluid leads to mode damping, and possibly modifies the Tkachenko mode functions, as in He II [3]. The analysis of the full three-dimensional problem will be published separately by S. A. Gifford and G. Baym.
- [24] Although the local superfluid velocity in a rotating fluid is irrotational, its long wavelength average is not [3].
- [25] To compute the sound velocity, one must take into account the correction to the interaction energy arising from the nonuniformity of the density around each vortex. As derived in [25], the interaction energy density is renormalized to  $g\bar{n}^2b/2$ , where  $\bar{n}$  is the mean density in a unit cell of the lattice, and  $b = \langle n^2 \rangle / \bar{n}^2 \gtrsim 1$ , a factor dependent on the density distribution in the cell. At low  $\Omega$ ,  $b = 1$ , while in the quantum Hall regime  $b = (e^2 - 5)/4(e - 2)^2 \approx 1.16$ . Neglect of the density dependence of  $b$  implies  $ms^2 = gnb$ , the result we use here.
- [26] U. R. Fischer and G. Baym, Phys. Rev. Lett. **90**, 140402 (2003); G. Baym and C. J. Pethick, cond-mat/0308325.
- [27] Including the higher order kinetic term,  $-\nabla^2 n/4m$ , in the pressure converts the linear spectrum,  $sk$ , into the full Bogoliubov spectrum,  $E_k = sk[1 + (k/2ms)^2]^{1/2}$ .
- [28] In three dimensions, the number of degrees of freedom remains four, since Eq. (1) now implies two constraints on the six degrees of freedom,  $n$ ,  $v$ , and  $\epsilon$ , and the system still supports only two long wavelength modes. As the wave vector becomes more aligned with the rotation axis, the Tkachenko mode tends to stiffen while the inertial mode tends to soften. In both modes the vortex motion remains elliptically polarized with the longitudinal component  $\approx -i\omega/2\Omega$  times the transverse component [23].
- [29] V. Schweikhard, I. Coddington, P. Engels, V. P. Mogendorff, and E. A. Cornell, cond-mat/0308582.